# Supplementary Information

# Reline Deep Eutectic Solvent as a Green Electrolyte for Electrochemical Energy Storage Application

Sara AZMI, Masoud FOROUTAN KOUDAHI and Elzbieta FRACKOWIAK *

Institute of Chemistry and Technical Electrochemistry, Poznan University of Technology,

Berdychowo 4, Poznan 60-965, Poland

* corresponding author: elzbieta.frackowiak@put.poznan.pl

**Table S1** Temperature dependence of electrical conductivity of Reline DES

| Temperature (T/ °C) | Conductivity (mS $cm^{-1}$) |
|---|---|
| 25 | 2.52 |
| 30 | 3.64 |
| 40 | 7.24 |
| 50 | 13.33 |
| 60 | 25.14 |
| 70 | 50.29 |
| 80 | 65.04 |
| 90 | 85.57 |
| 100 | 116.14 |
| 110 | 135.50 |
| 120 | 159.41 |
| 130 | 162.60 |
| 140 | 167.63 |
| 150 | 175.21 |

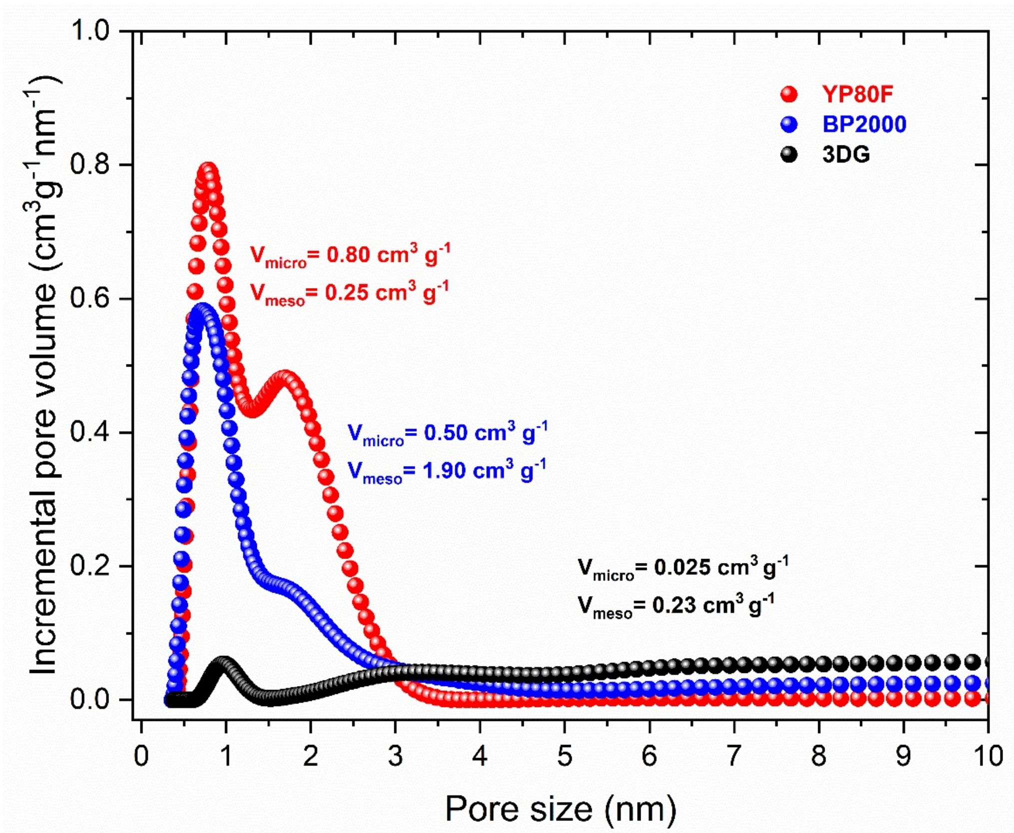


**Fig. S1** Pore size distribution of YP80F, BP2000 and 3DG materials

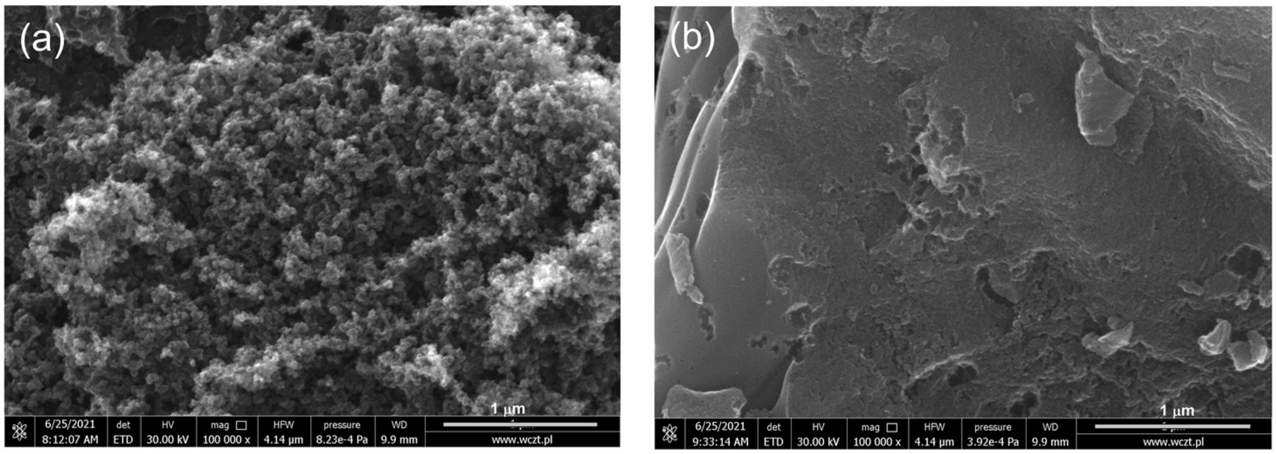


**Fig. S2** Scanning electron microscopy image of (a) BP2000; (b) YP80F

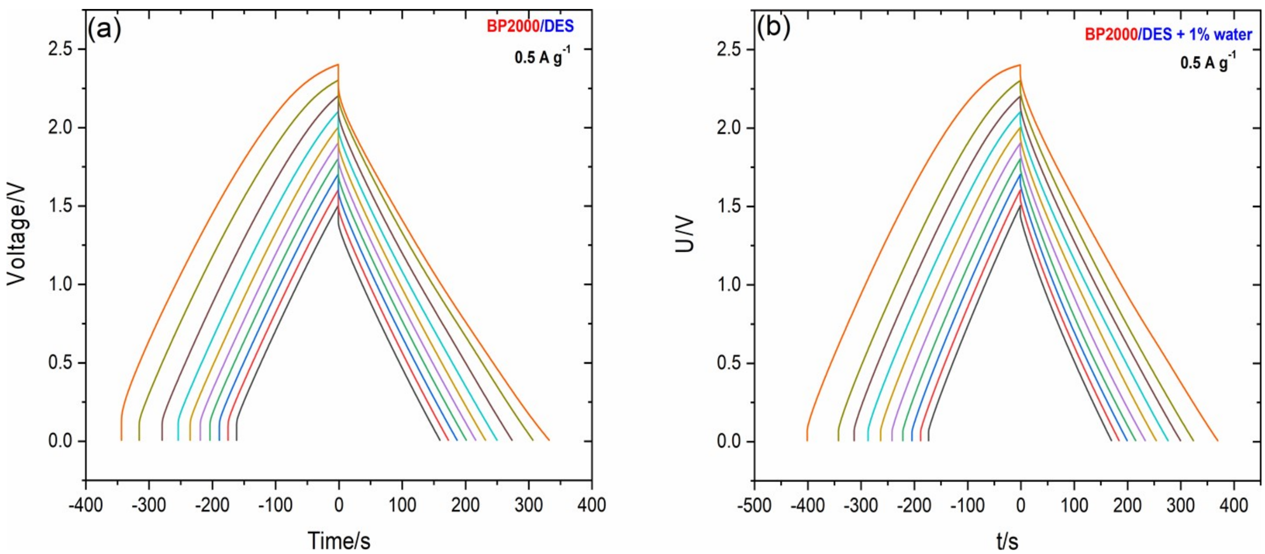


**Fig. S3** Galvanostatic charge/discharge profiles of the BP2000 based cells at different voltage limits ranging from 1.5 to 2.4V at 0.5 A $g^{-1}$ using (a) DES pure electrolyte; (b) DES+1% water electrolyte.

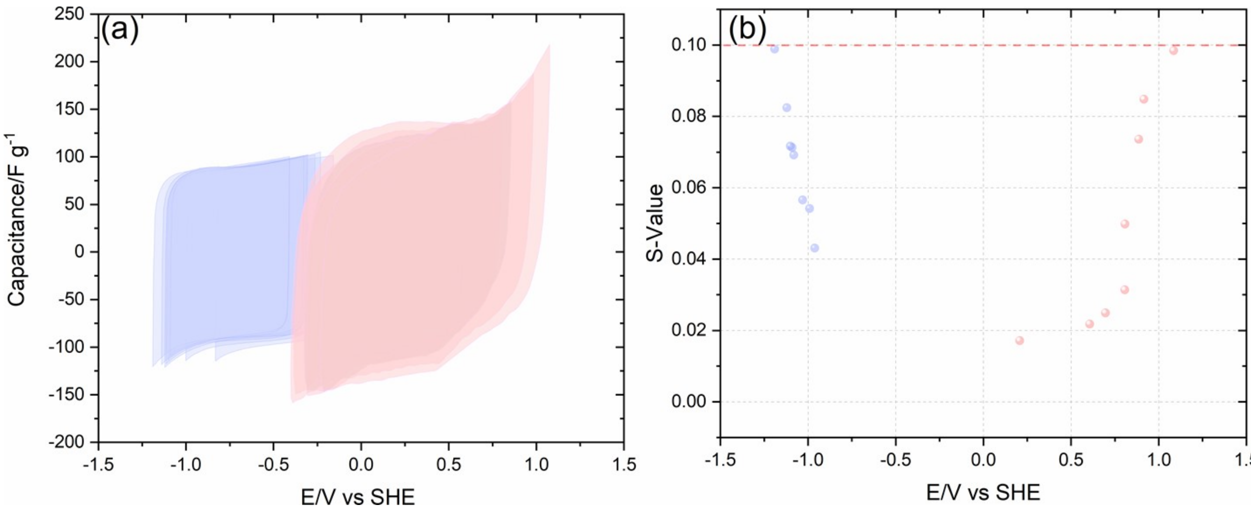


**Fig. S4** (a) Individual cyclic voltammograms and (b) corresponding S-value for (+) and (−) BP2000 electrodes in Reline DES electrolyte

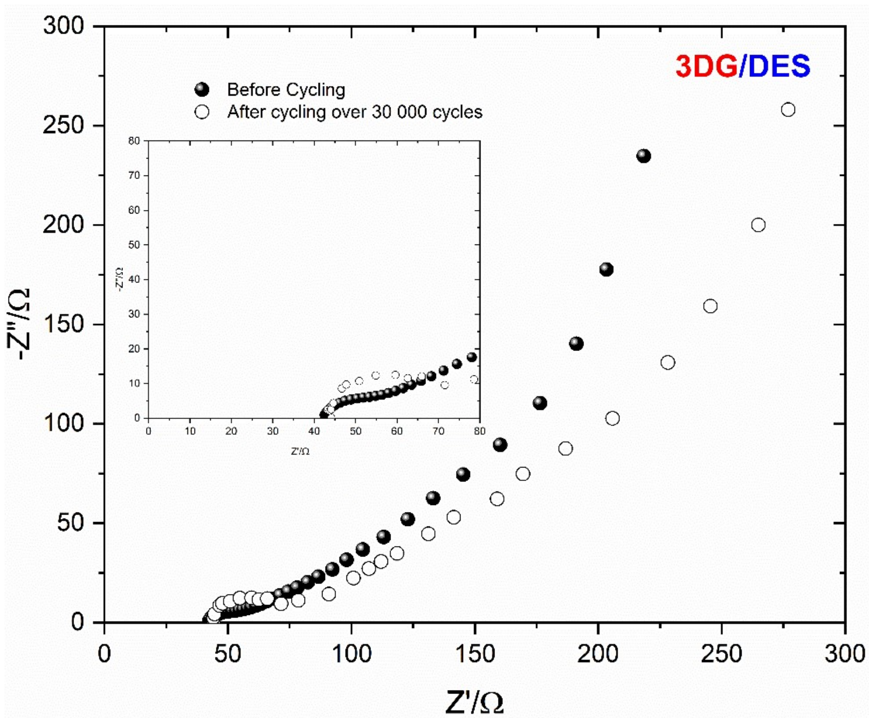


**Fig. S5** Electrochemical impedance spectroscopy plots for 3DG electrode based capacitor in Reline DES electrolyte before and after 30 000 cycles

Fig. S3 compares Nyquist plots before and after 30 000 cycles for 3DG based supercapacitor operating in Reline DES electrolyte. The inset low-frequency region displays a purely capacitive behaviour by the presence of a quasi-vertical line before and after cycling. Both insets show a relatively small Warburg region leading to a low ion diffusion impedance driving to a better charge propagation[1]. Before cycling, the equivalent series resistance value of Reline DES electrolyte was 42 Ω. Remarkably, after over 30 000 cycles, the ESR value remains almost the same (43 Ω).

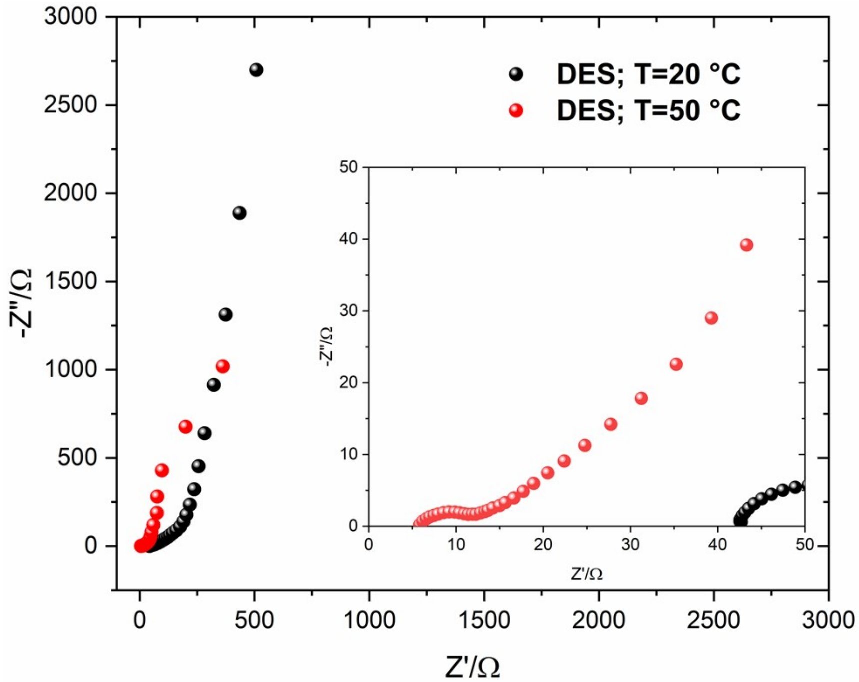


**Fig. S6** Electrochemical impedance spectroscopy plots for 3DG electrode based EC in Reline DES electrolyte

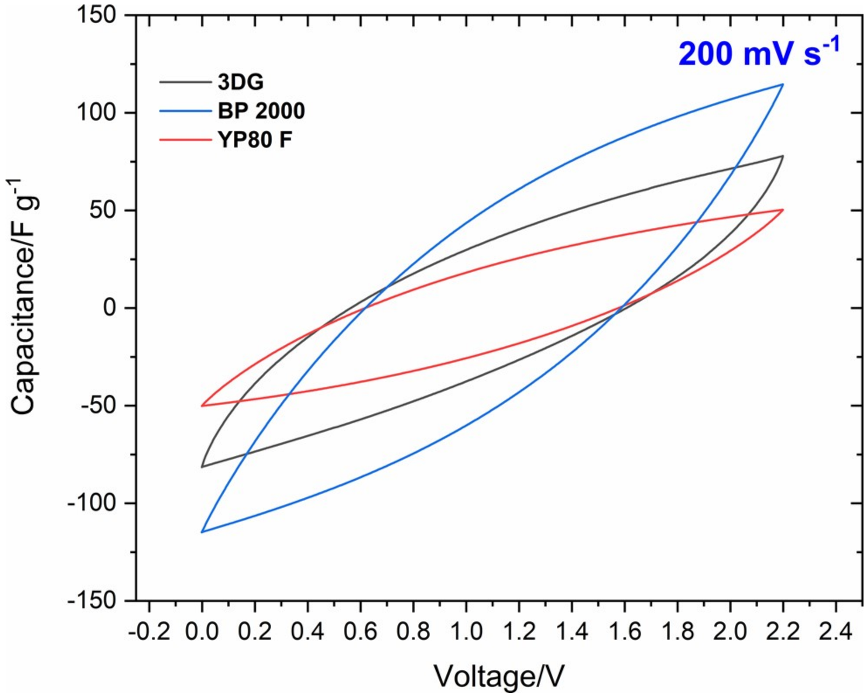


**Fig. S7** CV curves of 3DG, BP 2000 and YP 80F based capacitors at 200 mV $s^{-1}$.

Electrolyte Reline DES+1% water

**Table S2**: Comparison of the various DES based electrochemical capacitors.

| DES Electrolytes | | Cell voltage and operating temperature | Capacitance | Cycling Stability | Ref |
|---|---|---|---|---|---|
| **Electrolyte** | **Composition** | | | | |
| **Reline<br>Choline chloride (ChCl):Urea (U)** | ChCl:U (1:2) | 2.2V@25°C | 100 F g$^{-1}$@1 A g$^{-1}$ | <50 000@1 A g$^{-1}$ | **This work** |
| | ChCl:U (1:2) +1%wt $H_2O$ | 2.2V@25°C | 153 F g$^{-1}$@1 A g$^{-1}$ | <25 000@1 A g$^{-1}$ | |
| **Lithium bis[(trifluoromethyl)sulfonyl]imide (LiTFSI):Formamide (FMD)** | LiTFSI:FMD<br>(0.25:1) | 2V@25°C | 135 F g$^{-1}$@0.2 A g$^{-1}$ | 2000 at 2 A g$^{-1}$ | **2** |
| **Choline chloride (Chcl):Ethylene glycol (EG)** | ChCl:EG (1:1)<br>ChCl:EG (1:2)<br>ChCl:EG (1:4) | 2V@25°C | 53 F g$^{-1}$@4 A g$^{-1}$<br>102 F g$^{-1}$@4 A g$^{-1}$<br>61 F g$^{-1}$@4 A g$^{-1}$ | 10 000@4 A g$^{-1}$<br>10 000@4 A g$^{-1}$<br>10 000@4 A g$^{-1}$ | **3** |
| **N-methylacetamide (NMAc): LiX** | NMAc + LITFSI (1:0.25)<br>NMAc + $LIPF_6$ (1:0.25)<br>NMAc + $LINO_3$ (1:0.25) | 2.8V@80°C<br>2.0V@80°C<br>1.8V@80°C | 120 F g$^{-1}$@0.2 A g$^{-1}$<br>90 F g$^{-1}$@0.2 A g$^{-1}$<br>110 F g$^{-1}$@0.2 A g$^{-1}$ | 500 at 0.2 A g$^{-1}$<br>600 at 0.2 A g$^{-1}$<br>3000 at 0.2 A g$^{-1}$ | **1** |
| **N-methylacetamide (NMAc): lithium bis[(trifluoromethyl)sulfonyl]imide (LiTFSI)** | NMAc + LITFSI (1:0.25) | 2.5V@80°C | 152 F g$^{-1}$@20 mV s$^{-1}$ | not available | **4** |
| **Chitosan-supported Choline chloride (ChCl) :Lactic Acid (LA)** | ChCl:LA (1:2)<br>Chitosan:DES (1:4) | 1.6V@25°C | 194 mF cm$^{-2}$<br>@2 mA cm$^{-2}$ | 1500@2 mA cm$^{-2}$ | **5** |
| **N-methylacetamide:$NaNO_3$** | $NaNO_3$:MAc<br>(0.1:0.9) | 1.8V@80°C | 100 F g$^{-1}$@0.2 A g$^{-1}$ | 1000@0.2 A g$^{-1}$ | **6** |
| **Tetraethylammonium bromide (TEAB) or tetraethylammonium chloride (TEAC) and ethylene glycol (EG)** | TEAB:EG<br>(1:3)<br>(1:4)<br>TEAC:EG (1:5) | 1.8V@25°C | 102 F g$^{-1}$@1 A g$^{-1}$<br><br><br>100 F g$^{-1}$@1 A g$^{-1}$ | 10 000@1 A g$^{-1}$ | **7** |
| **N-methylacetamide (NMAc): lithium bis(fluorosulfonyl)imide (LiFSI)** | NMAc:LiFSI<br>(1:0.25) | 2V@25°C | 120 F g$^{-1}$@0.2 A g$^{-1}$ | not available | **8** |
| **N-methylacetamide (NMAc): sodium or bis(fluorosulfonyl)imide (NaFSI)** | NMAc:NaFSI<br>(1:0.10) | 1.5V@25°C | 130 F g$^{-1}$@0.2 A g$^{-1}$ | 5000@0.25 A g$^{-1}$ | |
| **Ethylene glycol (EG) and tetrapropylammonium bromide (TPABr)** | EG/TPABr<br>(1:5) | 1V@25°C<br>0.55V@115°C<br>0.65V@115°C | 100 F g$^{-1}$@0.1 A g$^{-1}$<br>135 F g$^{-1}$@0.1 A g$^{-1}$<br>172 F g$^{-1}$@0.1 A g$^{-1}$ | 10 000@0.25 A g$^{-1}$ | **9** |
| **Solid sulfonium bis[(trifluoromethyl)sulfonyl]imide (S111TFSI) aprotic ionic liquid formamide (FMD) and trifluoroamide (TFA)** | Protic ionic liquid<br>S111 TFSI (50%),<br>Trifluoroamide (50%)<br>and 1.0 M LiTFSI<br>Inert atm | 2.2V@80°C | 280 F g$^{-1}$@1 A g$^{-1}$ | 1000@0.25 A g$^{-1}$ | **10** |
| **Glyceline** | Glyceline | 1.5V@25°C | 173 mF cm$^{-2}$<br>@11 μA cm$^{-1}$ | 10 000@ 1 cm$^{-2}$ | **11** |
| **Choline chloride (ChCl) and butanediol** | ChCl: 1,2-butanediol<br>ChCl: 1,3-butanediol<br>ChCl: 1,4-butanediol<br>(1:4) | 2V@25°C<br>2V@25°C<br>2V@25°C | 116 F g$^{-1}$@4 A g$^{-1}$<br>101 F g$^{-1}$@4 A g$^{-1}$<br>65 F g$^{-1}$@4 A g$^{-1}$ | 10 000@4 A g$^{-1}$<br>10 000@4 A g$^{-1}$<br>10 000@4 A g$^{-1}$ | **12** |
| **Ethylene glycol (EG) and 1-butyl-3-methylimidazolium methanesulfonate ([BMIM]-[$MeSO_3$])** | [BMIM]-[$MeSO_3$]:EG<br>(1:3.5) | 2V@25°C | 55 F g$^{-1}$@0.3 A g$^{-1}$ | not available | **13** |
| **N-methylacetamide (NMAc) and 1-butyl-3-methylimidazolium methanesulfonate ([BMIM]-[$MeSO_3$])** | [BMIM]-[$MeSO_3$]:NMAc<br>(1:2) | 2V@25°C | 57 F g$^{-1}$@0.3 A g$^{-1}$ | not available | |

**SCs Characteristics Calculation methods**

The calculation methods were defined following Laheaar *et al*[14]. The capacitance ($C_{GC/GD}$) of the system was calculated from the slope of GCD curves using the following formula:

$$C_{GC/GD} = \frac{I\Delta t}{\Delta U} \qquad (F)$$

Where *I* is the applied current (A), *Δt* represents the discharge or charge duration (s) and *ΔU* is the cell potential (V). The capacitance values presented in this work are calculated for one electrode ($C_{el/GD}$) resulting from the next formula:

$$C_{el/GD} = \frac{2C_{GD}}{0.5\, m_{el}} \qquad (F\, g^{-1})$$

Where $m_{el}$ is the total mass of both electrodes.

The SC discharge energy ($E_{GD}$) as well as its specific energy ($E_{s,GD}$) can be calculated:

$$E_{GD} = \frac{C_{GD}\, U_{max}^{2}}{2} \qquad (W\, s)$$

$$E_{s,GD} = \frac{E_{GD}}{m_{el}\, 3.6} \qquad (Wh\, kg^{-1})$$

The capacitance derived from the discharge time ($C_{el/GD}$) was compared to the capacitance calculated by integrating the area under galvanostatic discharge curve ($C_{el,int/GD}$) which is directly related to the discharge energy ($E_{int/GD}$) calculated as follow:

$$E_{int/GD} = I \int_{t(U_{max})}^{t(U_{min})} U(t)dt \qquad (W\, s)$$

$$C_{int/GD} = \frac{2E_{int/GD}}{U_{max}^{2}} \qquad (F)$$

$$C_{el/int,GD} = \frac{C_{in/GD}}{0.5\, m_{el}} \qquad (F\, g^{-1})$$

The presented specific energy ($E_{s,int/DG}$) was calculated from the following formula:

$$E_{s,int/GD} = \frac{E_{int/GD}}{m_{el}\, 3.6} \qquad (Wh\, kg^{-1})$$

The coulombic efficiency ($\eta_t$) and the energy efficiency ($\eta_E$) of the SCs was evaluated from:

$$\eta_t = \frac{t_D}{t_C} \qquad (\%)$$

$$\eta_E = \frac{E_{\frac{int}{D}}}{E_{\frac{int}{C}}} \qquad (\%)$$

**References**

1 W. Zaidi, A. Boisset, J. Jacquemin, L. Timperman and M. Anouti, Deep Eutectic Solvents Based on *N* -Methylacetamide and a Lithium Salt as Electrolytes at Elevated Temperature for Activated Carbon-Based Supercapacitors*, J. Phys. Chem. C*, 2014, **118**, 4033–4042.

2 S. Phadke, S. Amara and M. Anouti, Gas Evolution in Activated-Carbon-Based Supercapacitors with Protic Deep Eutectic Solvent as Electrolyte, *ChemPhysChem*, 2017, **18**, 2364–2373.

3 M. Zhong, Q. F. Tang, Y. W. Zhu, X. Y. Chen and Z. J. Zhang, An alternative electrolyte of deep eutectic solvent by choline chloride and ethylene glycol for wide temperature range supercapacitors *, J. Power Sources*, 2020, **452**, 227847.

4 A. Boisset, J. Jacquemin and M. Anouti, Physical properties of a new Deep Eutectic Solvent based on lithium bis[(trifluoromethyl)sulfonyl]imide and N-methylacetamide as superionic suitable electrolyte for lithium ion batteries and electric double layer capacitors, *Electrochimica Acta*, 2013, **102**, 120–126.

5 V. K. Vorobiov, M. A. Smirnov, N. V. Bobrova and M. P. Sokolova, Chitosan-supported deep eutectic solvent as bio-based electrolyte for flexible supercapacitor*, Mater. Lett.*, 2021, **283**, 128889.

6 W. Zaidi, L. Timperman and M. Anouti, Deep eutectic solvent based on sodium cations as an electrolyte for supercapacitor application, *RSC Adv*, 2014, **4**, 45647–45652.

7 D. Wu, L. H. Xu, H. J. Feng, Y. W. Zhu, X. Y. Chen and P. Cui, Design and theoretical study of novel deep eutectic solvents: The effects of bromine and chloride anions on solvation structure and supercapacitor performance, *J. Power Sources*, 2021, **492**, 229634.

8 S. Amara, W. Zaidi, L. Timperman, G. Nikiforidis and M. Anouti, Amide-based deep eutectic solvents containing LiFSI and NaFSI salts as superionic electrolytes for supercapacitor applications*, J. Chem. Phys.*, 2021, **154**, 164708.

9 S. Sathyamoorthi, N. Phattharasupakun and M. Sawangphruk, Environmentally benign non-fluoro deep eutectic solvent and free-standing rice husk-derived bio-carbon based high-temperature supercapacitors, *Electrochimica Acta*, 2018, **286**, 148–157.

10 X. Baokou and M. Anouti, Physical Properties of a New Deep Eutectic Solvent Based on a Sulfonium Ionic Liquid as a Suitable Electrolyte for Electric Double-Layer Capacitors, *J. Phys. Chem. C*, 2015, **119**, 970–979.

11 F. Pettersson, J. Keskinen, T. Remonen, L. von Hertzen, E. Jansson, K. Tappura, Y. Zhang, C.-E. Wilén and R. Österbacka, Printed environmentally friendly supercapacitors with ionic liquid electrolytes on paper, *J. Power Sources*, 2014, **271**, 298–304.

12 L. H. Xu, D. Wu, M. Zhong, G. B. Wang, X. Y. Chen and Z. J. Zhang, The construction of a new deep eutectic solvents system based on choline chloride and butanediol: The influence of the hydroxyl position of butanediol on the structure of deep eutectic solvent and supercapacitor performance, *J. Power Sources*, 2021, **490**, 229365.

13 U. Mahanta, S. Choudhury, R. P. Venkatesh, S. Sarojini Amma, S. A. Ilangovan and T. Banerjee, *ACS Sustain.* Ionic-Liquid-Based Deep Eutectic Solvents as Novel Electrolytes for Supercapacitors: COSMO-SAC Predictions, Synthesis, and Characterization, *Chem. Eng.*, 2020, **8**, 372–381.

14 A. Laheaar, P. Przygocki, Q. Abbas, F. Beguin. Appropriate methods for evaluating the efficiency and capacitive behavior of different types of supercapacitors, *Electrochem. Commun.*, 2015, **60**, 21–25.